X-922-74-189
PREPRINT

NASA TM X- 70711

THE RELATION OF VARIATIONS IN TOTAL MAGNETIC FIELD AT HIGH LATITUDE WITH THE PARAMETERS OF THE INTERPLANETARY MAGNETIC FIELD AND WITH DP2 FLUCTUATIONS

R. A. LANGEL

JUNE 1974

GODDARD SPACE FLIGHT CENTER
GREENBELT, MARYLAND

For information concerning availability
of this document contact:

Technical Information Division, Code 250
Goddard Space Flight Center
Greenbelt, Maryland 20771

(Telephone 301-982-4488)

THE RELATION OF VARIATIONS IN TOTAL MAGNETIC FIELD AT HIGH LATITUDE WITH THE PARAMETERS OF THE INTERPLANETARY MAGNETIC FIELD AND WITH DP2 FLUCTUATIONS

R. A. Langel

Geophysics Branch
NASA Goddard Space Flight Center
Greenbelt, Maryland 20771

ABSTRACT

Distrubances in total magnetic field magnitude, ΔB, are generally positive from 2200 to 1000 magnetic local time (MLT) and negative from 1000 to 2200 MLT. The maximum disturbances from the positive and negative regions of ΔB (Bp and Bn, respectively) are investigated with respect to their correlation with 1) the average N-S component, Bz, 2) the average angle with respect to the solar magnetospheric equitorial plane, θ, 3) the variance, σ_i, and 4) the magnitude, Bi, of the interplanetary magnetic field. These quantities were averaged over a period, T, ranging from 20 min. to 8 hours prior to the measurement of Bp or Bn. In the correlation with Bz two methods were used: 1) direct correlation with Bz and 2) correlation with the sum $B_\Sigma = \Sigma B_z/T$ where $Bz < 0$. Bp vs. Bz showed the best correlation, -0.79, for T = 120 minutes. For Bn vs B_Σ, data were divided into an equinoctial and winter period. Maximum correlations of 0.63 at T = 200 minutes and 0.70 at T = 60 mintues were obtained for equinox and winter, respectively. In all cases the peak in the correlation coefficient, when plotted against T, was very broad. Correlations with all other parameters was smaller than for B_Σ. Examination of Bp as a function of average Bz shows that an approximately linear relation holds for $Bz < 0$ and that for $Bz > 0$, Bp is relatively constant. Significant magnitudes of ΔB are found to occur in both the positive and negative regions even when the interplanetary field has been northward for over an hour.

Comparison of the occurrence of disturbance in ΔB and in occurrence of DP2 fluctuations indicates no correlation between the two phenomenon.

Variations (i. e., disturbances) in total magnetic field magnitude have been studied (Langel, 1974a, b) utilizing data from the Polar Orbiting Geophysical Observatory satellites (OGO 2, 4, and 6), unofficially referred to as POGO. These data, from October 1965 through December 1969, covered the altitude range from 400-1510 km. Analysis is carried out in terms of the quantity ΔB, which is the measured field magnitude minus the field magnitude computed from a spherical harmonic analysis of the POGO data from especially chosen quiet days. The satellite, instrumentation, data accuracy, and details of the POGO (8/71) spherical harmonic analysis are given in earlier papers by Farthing and Folz (1967), Langel (1967, 1974a, b), Cain and Langel (1971), and Cain et al. (1967).

ΔB is found (Langel, 1974a) to be positive from near 22^h to near 10^h MLT (magnetic local time) and negative from near 10^h to near 22^h MLT. These regions are designated the positive ΔB region and the negative ΔB region, respectively. Figure 1 is a contour plot of average ΔB for one season, magnetic disturbance level, and altitude range. Both the positive and negative ΔB region are clearly discernible. This basic pattern prevails for all seasons and magnetic disturbance levels. Amplitude variations with altitude, season, and magnetic disturbance level are described in Langel (1974a). Variations with interplanetary magnetic sector are described in Langel (1974c).

Although the negative ΔB region can be accounted for in terms of ionospheric currents, this is not true for the positive ΔB region (Langel, 1974b). Some of the positive ΔB region disturbance is attributed to the ECS (equatorial current sheet = ring current) and some to the westward electrojet, but some data are not accounted for by this combination of sources. Equivalent ionospheric currents which could cause the variations in POGO data in the negative ΔB region (and also most of the surface ΔZ and ΔH in this local time region) were derived

by Langel (1974b) and denoted HLS (for High Latitude, Sunlit). HLS is a latitudinally broad current, as opposed to a jet-type current which has narrow (~3-6°) latitudinal extent, and is similar to the DPC current, proposed by Feldstein (1969) to account for high latitude surface magnetic variations on quiet summer days, and to the afternoon vortex of the DP2 current system proposed by Nishida and his co-workers (1966).

The purpose of this paper is to explore the relationships between variations in the ΔB as seen in the POGO data and variations 1) in the DP2 fluctuations reported by Nishida and co-workers and 2) in the N-S component, Bz, the variance, σ_i, and the magnitude, B_i of the interplanetary magnetic field. The southward component of interplanetary magnetic field ($Bz < 0$) has been found to be highly correlated with magnetic disturbance, particularly substorm activity (Arnoldy, 1971; Foster et al. 1971). Indeed, some workers (e.g. Coroniti and Kennel, 1972, 1973) believe that magnetospheric disturbances are generally initiated by a southward turning interplanetary magnetic field. Burch (1973) found that the latitudes of the poleward and equatorial boundaries of the magnetospheric cusp region could be ordered according to the average value of Bz or the average value of θ for some period prior to the boundary measurement. This ordering was much better for Bz than for θ and for a period of 45 min. prior to the boundary measurement rather than 15, 30, or 60 min.

This study will show that detailed correlation between the interplanetary parameters and the disturbance magnitude at POGO is not present on individual passes but that statistical correlations between disturbance magnitudes in both the negative and positive ΔB regions do exist. Also, no correlation is found between ΔB at POGO and the occurrence of DP2 fluctuations.

RELATION WITH PARAMETERS OF THE INTERPLANETARY MAGNETIC FIELD

Statistical correlations. For each individual pass the following parameters are defined:

B_n: the minimum ΔB in the negative ΔB region.

B_p: the maximum ΔB in the positive ΔB region.

Associated with each B_n or B_p are the following:

B_Σ (T) = $\Sigma B_z/T$ for the interplanetary field points where $B_z < 0$.

$\langle B_z\ (T)\rangle$: the average value of B_z

$\langle \theta\ (T)\rangle$: the average angle of the interplanetary field with respect to the solar magnetospheric equatorial plane,

$\langle \sigma_i^2(T)\rangle$: the average variance of the interplanetary magnetic field

$\langle B_i\ (T)\rangle$: the average magnitude of the interplanetary field

The sum B_Σ (T) and the various averages are taken over a time span of T minutes prior to the time of measurement of B_n or B_p. All interplanetary field parameters are computed from Explorer 34 twenty second average data in the solar magnetospheric coordinate system. For these studies, POGO data were restricted to altitudes below 550 km for B_n, to minimize effects of altitude variations, add to altitudes above 700 km for B_p, to minimize the effects both of altitude variations and of the electrojet currents.

Correlation coefficients have been computed for $20 \leq T \leq 480$ minutes. First consider the positive ΔB region. The computations with B_z have been carried out three ways, first with data at all times up to T minutes prior to the time of B_p second, omitting the data within 10 minutes of the time of B_p and third, omitting the data within 20 minutes of the time of B_p. In all cases the

maximum correlations occurred for T = 120 min. Only small differences occurred between the three methods of data selection. Figure 2 shows the correlation coefficient, R, between B_Σ and B_p as a function of T for the second method of data selection. R is less than -.6 from T = 40 min. to 480 min. with a very broad peak of -0.786 at T = 120 min. R for $B_p - \langle\theta\rangle$ and $B_p - \langle B_z\rangle$ is -.48 and -.69 at the maximum (cf. Table 1) and in both cases has a broad peak similar to that for $B_p - B_\Sigma$. The broadness of this peak indicates that whatever magnetospheric phenomena is causing the near earth positive ΔB is affected to some extent by southward B_z as far as 8 hours in the past. Study of B_Σ as a function of time for individual measurements of B_p confirms this. In some cases of large B_p, B_Σ is relatively high for $T < 120$ min. and decreasing thereafter, implying that the interplanetary field-magnetospheric interaction is higher for $T < 120$ min. In other cases, with B_p of comparable magnitude, B_Σ becomes larger in magnitude with increasing time, in some cases reaching its maximum at T = 480 min. The significance of the observed correlations may be tested by calculation of the probability that such a correlation could arise, by random sampling, from an uncorrelated population. This test is accomplished by use of the t-distribution (Fisher, 1958). For the present case, t is given by

$$t = \frac{R \cdot \sqrt{N - 2}}{\sqrt{1 - R^2}}$$

where N is the number of pairs of observations. For B_p vs. B_Σ the probability of obtaining the correlation coefficients of Figure 2 from an uncorrelated population is below 0.1 for $20 \leq T \leq 480$ min. and is below 0.06 for $120 \leq T \leq 240$ min. Thus a great deal of significance should be attached to this correlation.

For B_p vs $\langle\theta\rangle$, this probability is always above 0.25 and reaches 0.5 at T = 480 minutes. For B_p vs. $\langle B_z\rangle$ the probability is between 0.14 and 0.33. The correlations of B_p with $\langle B_z\rangle$ and, especially, with $\langle\theta\rangle$ are much less significant than that with B_Σ.

It is instructive to examine plots of B_p vs. B_Σ, $\langle B_z\rangle$, and $\langle\theta\rangle$. These are given in Figure 3 for T = 120 min. In all cases there is a great deal of scatter. B_p vs. B_Σ is relatively linear and a least squares fit to the 68 data points in Figure 3a gives:

$$B_p = 17.75 - 8.15\, B_\Sigma(\gamma). \tag{1}$$

The standard deviation to this fit is 23.3γ. As expected, the minimum standard deviation occurs for the same T as the maximum $|R|$. There are a large number of points for which $|B_\Sigma|$ is small and B_p is large (> 20 or 30γ). This is reflected in the fit to the data which gives $B_p \doteq 18\gamma$ for $B_\Sigma = 0$. Some disturbance can occur when the interplanetary field has been northward for some time. Figures 3b and 3c show B_p vs. $\langle B_z\rangle$ and $\langle\theta\rangle$, respectively. In both cases the plot characteristics change as the average field direction goes from south to north. Two hand-drawn lines are shown in Figure 3b to illustrate this effect. Thus there is a clear statistical difference in the magnetospheric response, in this case B_p, to southward and northward fields. The scatter in both of these plots is large and it is larger for $\langle\theta\rangle$ than for $\langle B_z\rangle$ which implies that the magnitude of the southward component is more important than the field angle with respect to the solar magnetospheric equatorial plane. A similar difference in the response of the equatorward boundary of the dayside cusp to variations in B_z between northward and southward B_z was found by Burch (1973). Between

$B_z = 0$ and $B_z = -6\gamma$ this boundary moves equatorward by 5° whereas between $B_z = 0$ and $B_z = 6\gamma$ this boundary moves poleward only 1.5°. The statistical results presented for B_p are summarized in Table 1 along with the rest of the statistical results of this study. All data used in this study are from the northern hemisphere.

Negative ΔB Region. Seasonal effects are large in the negative ΔB region so available data from this region are divided into two seasonal groups, an early equinoctial period from August 5 to September 10, 1967, and a winter period from November 5 to December 15, 1967. Because the level of negative ΔB is much lower in the winter, and because the number of data points available for winter (35) is lower than for equinox (88), care should be made when comparing the seasons or drawing conclusions based on analysis of the winter data. Figure 4 shows the correlation coefficients for B_n vs. B_Σ as a function of T. As for the positive ΔB region, the peak of each curve is very broad. For the equinox data R reaches 0.63 at T = 200 minutes and for the winter data R reaches 0.70 at T = 60 minutes. The probabilities for obtaining these results from an uncorrelated population are very small. For the equinox data the probability is always less than 0.025, and usually less than 0.02, for $20 \leq T \leq 480$ min. For the winter data the probability is always less than 0.036. Plots of B_n vs. B_Σ are shown in Figure 5. Least squares fits to these data yield

$$B_n = -44.0 + 8.05\, B_\Sigma(\gamma) \qquad (2)$$

with a standard deviation of 27.1 γ, for the equinox data and

$$B_n = -21.7 + 3.4\, B_\Sigma(\gamma) \qquad (3)$$

with a standard deviation of 14.8γ, for the winter data. The scatter for the equinox data is very large, larger than was found in the positive ΔB region, and the scatter for the winter data is smaller but still significant. As for the positive ΔB regions, a considerable number of points occur for which $|B_\Sigma|$ is small and $|B_n|$ is large. Equations (2) and (3) both indicate that considerable disturbance is expected even when the interplanetary field has been northward for some time.

Other Interplanetary Parameters. Garrett (1974) has shown that fluctuations in the interplanetary magnetic field (e.g. measured by the variance of the field fluctuations, σ_i^2) play a role in determining the magnitude of substorm activity. Another candidate interplanetary field parameter for correlation with magnetospheric disturbance phenomena is the magnitude, B_i, of the interplanetary field. Because of the dominance of the correlation of B_p and B_n with B_Σ, and because the temporal relation between σ_i^2, B_i, or B_Σ and B_p or B_n may be different, the correlations found between σ_i or B_i and B_p or B_n are not as conclusive as the correlation between B_Σ and B_p or B_n. Computation of the correlation coefficient, R, between $\langle\sigma_i^2\rangle$ or $\langle B_i\rangle$ and B_p or B_n was carried out in the same manner as the computation between B_Σ and B_p or B_n and the results are summarized in Table 1. The correlation coefficients have somewhat greater magnitudes in the positive ΔB region than in the negative ΔB region but it is not clear that this is a significant difference. If it is significant, the difference may be a reflection of the different sources of disturbance, i.e. ionospheric for the negative ΔB and mostly non-ionospheric for the positive ΔB (esp. at these altitudes, > 700 km).

For completeness, the coefficients C_n in

$$B_p = C_1 B_\Sigma(T_1) + C_2 \cdot \langle\sigma_i^2(T_2)\rangle + C_3 \cdot \langle B_i(T_3)\rangle \qquad (4)$$

were determined by least squares. T_n is taken to be the time of maximum correlation coefficient for the corresponding variable. The correlation coefficient of B_p computed from (4) with the measured B_p, and the σ of the fit are given in Table 1. Some improvement in the representation of B_p or B_n is obtained in each case.

Most of the computations described were repeated for subsets of the data to check for bias in data selection. No such bias was found. In particular, data subdivided by interplanetary magnetic sector showed no sector differences considered to be statistically significant.

Examples from Individual Satellite Passes. It is particularly noteworthy that both B_p and B_n can be large when B_z has been northward for some time. Several passes have been chosen to illustrate this point further. Two such passes, together with the pertinent B_z, are shown in Figure 6. In the top figure (7/29/67), B_z has been northward for several hours and nearly constant for about one hour, yet both positive and negative ΔB regions show peak $|\Delta B|$ greater than 50 γ. In the bottom figure (8/11/67), B_z fluctuates more than in the top figure but is still quite positive for about 1.5 hours prior to the pass. ΔB in the positive ΔB region reaches only $\sim 35\ \gamma$, but the satellite track does not pass through the MLT where maximum ΔB generally occurs. Although there is a data gap in the negative ΔB region, it is still clear that $|\Delta B|$ reached at least 40γ.

Although the statistical correlation of B_p and B_n with B_Σ and B_z is clear, pass by pass correlation with B_z is not clear. This is illustrated by Figure 7 which gives a time history of B_z and of the POGO data for 31 hours on August 12-13, 1967. The satellite passes are numbered 1-9 and the times of these passes indicated on the B_z plot. Disturbance in both the positive and the negative ΔB

regions is present in all cases, although the magnitude of ΔB varies considerably, but since the satellite track does not cover the same MLT in each case, detailed comparison of ΔB magnitude is not attempted.

B_z is southward until 1^h UT on 8/12, at which time it swings north and, after some agitation, settles down to a positive value from about 2.5 - 5.8^h UT. Pass 1 occurs during a southward period for B_z in the period of agitation, and both positive and negative ΔB are high ($|\Delta B|$ max $\sim 80\gamma$). Pass 2 occurs after B_z has been northward for more than 30 min., and $|\Delta B|$ is lower in both regions, although the change in positive ΔB is greater than in negative ΔB. From 6^h to 18.5^h UT on 8/12, B_z is mainly northward but is quite agitated. Pass 3 occurs during this period, and ΔB is significant in both regions and, in fact, is stronger than in pass 2. Perhaps the disturbance level here is influenced by the amount of variation as well as by the direction of B_z (cf. Garrett, 1974). From $19-22^h$ UT B_z is southward, although the magnitude of B_z is not large ($\sim 1.5\gamma$). Passes 4-6 are from this period, and $|\Delta B|$ in both regions shows a small but definite increase as time progresses, as expected from the discussion of Figure 2. Although $B_z < 0$ during and before pass 4, and $B_z > 0$ during and before pass 3, the disturbance level for both regions is higher during pass 3 than during pass 4. B_z is northward from just before 23^h UT on 8/12 to about 15 min. into 8/13, when it becomes agitated and, mainly, southward. Pass 7 occurs just after B_z has turned southward, and both regions show strong $|\Delta B|$. $|\Delta B|$ in pass 8 is large in both regions (note the scale change to 150γ) although the southward B_z is small in magnitude. Again, the variation in B_z might increase the disturbance level. Pass 9 occurs after B_z has been northward for about 2^h,

but with a significant amount of agitation. Disturbance in the negative ΔB region is small ($\sim -25\gamma$) although ΔB in the positive ΔB region reaches 60γ, which is as large as for those passes (4, 5, 6, 7, 8) where $B_z < 0$.

Discussion. A close correlation between instantaneous B_z and $|\Delta B|$ does not occur. Correlation between ΔB and B_z history for about 30 min. to several hours prior to the ΔB measurement is strong, and, possibly, some correlation with the interplanetary field magnitude and its degree of variation. A correlation exists with the amount of southward field for the previous 8 hours, at least. The time constants of 30-60 min. found between B_z and substorms are shorter than those found in the present study. If time constants are to be assigned, and because of the broadness of the peaks of R (cf. Figures 3 and 4), and because the interplanetary field parameters are averaged for T minutes and not instantaneous, it is not clear that this is meaningful, the times in Table 1 might be appropriate (although, since quantities are averaged for T minutes, T/2 might also be appropriate). The time constant associated with B_Σ, i.e. the effects of southward B_z, is 120 minutes for positive ΔB and 200 minutes for negative ΔB in equinox. The value of 60 minutes obtained for winter in the negative ΔB region may indicate a seasonal dependence but should be treated with caution because of the low amplitude of the negative ΔB in winter and the poor statistics compared to the other computations. The times associated with $\langle \sigma_i^2 \rangle$ and $\langle B_i \rangle$ are not as well determined as those associated with B_Σ because the variation of R as a function of T is much less for these variables. In particular, the value of 440 minutes for $\langle B_i \rangle$ in the positive ΔB region is not well determined.

That the time constants found for the correlations of interplanetary parameters with ΔB are greater than those found by previous workers between

southward B_z and substorm activity does not contradict these earlier results because Langel (1974b) found that the major sources of ΔB were separate from the electrojet currents but that there is a tendency for the Δ B magnitude to be high during periods of substorm activity.

Although it is magnetospheric rather than ionospheric in origin, the high latitude positive ΔB is not predicted by the most recent theoretical field models (Sugiura and Poros, 1973; Olson, 1972; Olson and Pfitzer, 1973). These models are also deficient in their representation of ΔB near the magnetopause in day-side high latitudes (i.e. near the cusp). Sugiura and Poros (1973) point out that this seems to indicate deficiencies in the theoretical model for the magnetopause currents. They also point out that the theoretical models do not include the current system associated with the polar cusp which is likely to have a substantial affect on ΔB at high latitudes. It is not known if a correct theoretical description of the magnetic fields beyond 2Re will also provide an explanation of the near earth positive ΔB.

RELATION WITH DP2

The DP2 Current System. Nishida and co-workers (1966) noted that certain fluctuations in polar cap and equatorial magnetic field occur in-phase. Analysis of such data (see also Nishida, 1968a, b, 1971; Nishida and Maezawa, 1971) led these workers to identify these disturbances with S_q^p except that they noted that the disturbance is worldwide and not confined to the polar cap. These workers also stress a high correlation between DP2 and the southward component of the interplanetary magnetic field. DP2 is supposed to have a peak-to-peak correspondence with the southward field with a time lag of 10-20 min. for disturbances of duration near 1 hr. Auroral electrojet activity, in this notation, is

called DP1. Nishida and Kokubun (1971) claim that, for Kp greater than about 4, DP2 becomes less evident and DP1 dominates. DP1 and DP2 are not seen to be mutually exclusive, Iijima and Nagata (1968, 1972) and Kokubun (1971, 1972) find that DP2 or SP activity precedes DP1 activity by one to two hours; they identify DP2 with a growth phase for magnetic substorms.

Relation Between Satellite ΔB and DP2. A DP2 current system would cause negative and positive ΔB in the negative and positive ΔB regions, respectively, which raises questions concerning the correlation of DP2 with the POGO ΔB measurements. In particular, (1) could DP2 be responsible for some of the disturbance in the positive ΔB region (in addition to the ECS and westward electrojet), and (2) is HLS a part of the DP2 current system? An attempt has been made to relate instances of DP2 with the satellite ΔB. As an example, Figure 8 shows B_z (interplanetary N-S component), X and Y from AT, and H from a selected group of low latitude observatories. (Table 2 gives observatory mnemonics and locations.) According to Nishida and co-workers, DP2 consists of simultaneous fluctuations in X and Y at polar cap stations (such as AT) and H at low latitude observatories. Most examples cited utilize an equatorial observatory at dawn to dusk local times. These fluctuations are supposed to be correlated with fluctuations in B_z. In Figure 8, 20 "fluctuations" are noted in the X and Y components at AT, as indicated by the shaded portions labeled A, B, etc. Fluctuations in B_z and low latitude H, which we felt correlated in a reasonable manner with the fluctuations at AT, are also shaded and labeled. Some fluctuations in data from AT occur which we have not considered; these generally do not correlate well with the other data. Local times of 6^h, 12^h,

18^h , and 24^h are indicated for each low latitude observatory as DA, N, DU, and M, respectively.

Of the 29 examples correlation with B_z is found for 20 cases (A, B, D, E, F, H, I, J, K, L, M, N, P, Q, R, S, T, W, AB, AC). Of the other 9 examples, 3 do not have the characteristics of DP2 at low latitudes (X, Y, AA), 5 are either weak and/or only seen at one or two stations at low latitudes (G, O, U, V, Z), and one (C) has all of the characteristics of DP2.

For the 20 cases where B_z is correlated with data from AT, 7 are either weak and/or only seen at one or two stations at low latitudes (M, N, P, R, T, U, V,), and 2 (F, V) have low latitude fluctuations which are not simultaneous with the AT data.

Although an extensive discussion of the nature and reality of DP2 is not attempted, several comments resulting from the study of this and other time periods are appropriate. First, it is extremely difficult, and seemingly somewhat arbitrary, to choose "fluctuations" which meet the criteria for DP2. Second, fluctuations occur frequently in all of the data involved, and it is unclear that the supposed DP2 are more than coincidence, at least for the data we have considered. The occurrence of examples C, G, O, U, V, and Z, which show many of the characteristics of DP2 but do not correlate with B_z, lend weight to the idea of coincidence in unrelated fluctuations, as does the occurrence of cases like M and N which are seen only weakly at one low latitude station although B_z and X component at AT correlate well (see also Onwumechili et al., 1973, for further comments of the nature of DP2).

Assuming that DP2 does exist, and is identified as the 20 examples where B_z correlates with data from AT, consider the relation with simultaneous

POGO data. The time period under consideration is the same as that of Figure 7, and the times of the nine satellite passes are indicated on Figure 8 by numbered arrows. Pass 1 occurs during a high level of substorm activity and will not be considered in the correlation. From 3^h UT on the 12th to 8^h UT on the 13th substorm activity is low and should not mask any DP2 present. A summary of results is given in Table 3.

In passes 3, 5, and 9 an additional source(s), besides the westward electrojet and the ECS, is necessary to account for the positive ΔB (see Langel, 1974a). None of these passes occur during an apparent DP2 event, although passes 3 and 5 occur during other types of fluctuations in X at AT. Three passes (4, 8, and 9) occur during periods when DP2 is certainly absent, yet both positive and negative ΔB are evident in the POGO data. On pass 8 very large magnitudes of ΔB occur in both regions. Only on pass 7 is there a case of DP2 occurrence at a time of significant ΔB.

On the basis of these and other data where significant ΔB is present in the absence of DP2 fluctuations, no correlation between the DP2 fluctuations and the ΔB at POGO is found, and it is concluded that HLS is not a portion of the current system associated with DP2 fluctuations as defined by Nishida and his co-workers. Although no correlation is found with DP2 fluctuations, estimates of non-electrojet positive ΔB are not so well determined that a positive ΔB contribution from a current of the DP2 type can be excluded. Such a current would, of course, not be associated with "DP2 fluctuations," as shown above, and would not be a dominant source, as shown by Langel (1974b).

ACKNOWLEDGEMENTS

I would like to thank D. Fairfield for the use of Explorer 34 data and J. Burch for critical review of the manuscript resulting in valuable suggestions.

REFERENCES

Arnoldy, R. L., Signature in the interplanetary medium for substorms, J. Geophys. Res., 76, 5189, 1971

Burch, J. L., Rate of erosion of dayside magnetic flux based on a quantitative study of the dependence of polar cusp latitude on the interplanetary magnetic field, Radio Sci., 8, 955-961, 1973

Cain, J. C., R. A. Langel, and S. J. Hendricks, First magnetic field results from the OGO-2 satellite, Space Res., VII, 1467, 1967

Cain, J. C. and R. A. Langel, Geomagnetic survey by the Polar Orbiting Geophysical Observatories, World Magnetic Survey, ed. A. J. Zmuda, IAGA Bull. No. 28, Paris, 1971

Coroniti, F. V., and C. F. Kennel, Changes in magnetospheric configuration during the substorm growth phase, J. Geophys. Res., 77, 3361, 1972

Coroniti, F. V., and C. F. Kennel, Can the ionosphere regulate magnetospheric convection, J. Geophys. Res., 78, 2837, 1973

Farthing, W. H. and W. C. Folz, Rubidium vapor magnetometer for near earth orbiting spacecraft, Rev. Sci. Instr., 38, 1023-1030, 1967

Feldstein, Y. I., Polar auroras, polar substorms, and their relationships with the dynamics of the magnetosphere, Rev. Geophys., 7, 179-218, 1969

Fisher, R. A., Statistical Methods for Research Workers, Hafner, New York, 1958

Foster, J. C., D. H. Fairfield, K. W. Ogilvie and T. J. Rosenberg, Relationship of interplanetary parameters and occurrence of magnetospheric substorms, J. Geophys. Res., 76, 6971, 1971

Garrett, Henry B., The role of fluctuations in the interplanetary magnetic field in determining the magnitude of substorm activity, to be published in Planet. Space Sci., 1974

Iijima, T., and T. Nagata, Constitution of polar magnetic disturbances, Rep. Ionos. Space Res. Japan, 22, 1, 1968

Iijima, T., and T. Nagata, Signatures for substorm development of the growth and expansion phase, Planet. Space Sci., 20, 1095-1112, 1972

Kokubun, S., Polar substorm and interplanetary magnetic field, Planet. Space Sci., 19, 697-714, 1971

Kokubun, S., Relationship of interplanetary magnetic field structure with development of substorm and storm main phase, Planet. Space Sci., 20, 1033-1049, 1972

Langel, R. A., Processing of the total field magnetometer data from the OGO-2 satellite, NASA/GSFC Report X-612-67-272, Goddard Space Flight Center, Greenbelt, Md., June 1967

Langel, R. A., Near earth magnetic disturbance in total field at high latitudes; I. summary of data from OGO's 2, 4, and 6, J. Geophys. Res., in press 1974a

Langel, R. A., Near earth magnetic disturbance in total field at high latitudes; II. interpretation of data from OGO's 2, 4 and 6, J. Geophys. Res., in press, 1974b

Langel, R. A., Variation with interplanetary sector of the total magnetic field measured at the OGO - 2, 4, and 6 satellites, to be published in Planet. Space Sci., 1974c

Nishida, A., Geomagnetic DP2 fluctuations and associated magnetospheric phenomena, J. Geophys. Res., 73, 1795, 1968a

Nishida, A., Coherence of geomagnetic DP2 fluctuations with interplanetary phenomena, J. Geophys., Res., 73, 5549, 1968b

Nishida, A., DP2 and polar substorm, Planet. Space Sci., 19, 1971

Nishida, A., N. Iwasaki, and T. Nagata, The origin of fluctuations in the equatorial electrojet: a new type of geomagnetic variation, Ann. Geophys., 22, 478, 1966

Nishida, A., and K. Maezawa, Two basic modes of interaction between the solar wind and the magnetosphere, J. Geophys. Res., 76, 2254, 1971

Nishida, A., and S. Kokubun, New polar magnetic disturbances, S_q^p SP, DPC, and DP2, Rev. Geophys. Space Phys., 9, 417, 1971

Onwumechili, A., K. Kawasaki, and S. I. Akasofu, Relationships between the equatorial electrojet and polar magnetic variations, Planet. Space Sci., 21, 1-16, 1973

Sugiura, M. and D. J. Poros, A magnetospheric field model incorporating the OGO 3 and 5 magnetic field observations, Planet. Space Sci., 21, 1763-1773, 1973

Olson, W. P., Distributed magnetospheric currents and their magnetic effects (abstract). EOS, Trans. Am. Geophys. Un., 53, 1089, 1972

Olson, W. P., and K. A. Pfitzer, Magnetospheric boundaries and fields, McDonnell Douglas Astronautics Company Paper WD 2173, 1, 1973

TABLE 1: CORRELATIONS WITH INTERPLANETARY MAGNETIC FIELD PARAMETERS

		B_Σ	$\langle B_z \rangle$	$\langle \theta \rangle$	$\langle B_i \rangle$**	$\langle \sigma_i^2 \rangle$**	B_p^{c*}
BP	Maximum Correlation Coefficient, R	-0.79	-0.69	-0.48	0.58	0.48	0.83
	Time of Maximum R (minutes)	120	80	80	440?	280	---
	Standard deviation of fit (γ)	23.3	33	41	51	54	20.8
BN Equinox	Maximum Correlation Coefficient, R	0.63	0.54	0.57	-0.42	-0.29	0.69
	Time of Maximum R (minutes)	200	80	80	40	20	---
	Standard deviation of fit (γ)	27	29	29	82	79	25
BN Winter	Maximum Correlation Coefficient, R	0.70	0.59	0.59	-0.35	-0.13	0.75
	Time of Maximum R (minutes)	60	100	40	10	80	---
	Standard deviation of fit (γ)	14.8	16.7	16.9	43	41	13.6

*$B_p^c = C_1 \cdot B_\Sigma(T_1) + C_2 \cdot \langle \sigma_i^2(T_2) \rangle + C_3 \cdot \langle \bar{B}_i(T_3) \rangle$, where T_1, T_2 and T_3 are the times of maximum R and the C_N, are determined by least squares

**For $\langle B_i \rangle$ and $\langle \sigma_i^2 \rangle$, R and σ varied very little for $0 < T < 480$ minutes.

TABLE 2. LOW LATITUDE OBSERVATORIES UTILIZED FOR DP2 DETERMINATION

Station	Mnemonic	Geographic Coordinates		Geomagnetic Coordinates		Station	Mnemonic	Geographic Coordinates		Geomagnetic Coordinates	
		Lat.	Long.	Lat.	Long.			Lat.	Long.	Lat.	Long.
Bangui	BA	4°26'	18°34'	4.8°	88.4°	Yangi-Bazar	YB	41°20'	69°37'	32.3°	144.0°
Gnangara	GN	41°20'	69°37'	32.3°	144.0°	Guam	GU	13°35'	144°52'	3.9°	212.8°
Honolulu	HO	21°19'	-158°.1'	21.0°	266.4°	Tucson	TU	32°15'	-110°50'	40.4°	312.2°
San Juan	SJ	18°6.8'	-66°9'	29.6°	3.1°	Paramaribo	PA	5°49'	-55°13'	16.9°	14.3°
M'Bour	MB	14°23'	-16°58'	21.2°	55.0°						

TABLE 3. CORRELATION OF DP2-LIKE VARIATIONS AND ΔB AT POGO

Pass #	Maximum Positive ΔB (γ)	Maximum Magnitude of Negative ΔB (γ)	Dst (γ)	DP2 Correlation
2	30	55	-12	During event C, magnetic disturbance like DP2, no Bz correlation
3	65	65	-2	During fluctuation in X at AT with no corresponding low-latitude H fluctuations.
4	38	50	-4	Quiet period in all data, no DP2, although Bz < 0.
5	42,62	80	-7	During event V, not a DP2 event.
6	70	70	-10	During fluctuation in X at AT lasting about 1^h. No correlated fluctuations in low latitude H or in Bz although Bz < 0. This event does not meet criteria for DP2.
7	30	70	-14	During event W, which is a DP2 event.
8	50	103	-10	Quiet pass in all data, although Bz < 0.
9	60	25	0	Quiet period following event AB (not a DP2 event).

FIGURE CAPTIONS

Figure 1 Average ΔB from OGO 2, 4 and 6. Data is from months 3, 4, 9, and 10, the northern hemisphere, and is at altitudes less than 550 km. Kp was 2- to 3+. Coordinates are magnetic local time and dipole latitude.

Figure 2 Correlation coefficient of B_p vs. B_Σ (T) as a function of T.

Figure 3 a) B_p vs. B_Σ. B_Σ is for T = 120 min. Dashed line is best fit to data in a least squares sense. b) B_p vs. $\langle B_z \rangle$. $\langle B_z \rangle$ is for T = 120 min. The dashed lines are hand drawn to illustrate the change in behavior for $\langle B_z \rangle > 0$ and $\langle B_z \rangle < 0$. c) B_p vs. $\langle \theta \rangle$. $\langle \theta \rangle$ is for T = 120 min.

Figure 4 Correlation coefficients of B_n vs. B_Σ(T) as a function of T. a) is for an equinoctial period and b) is for a winter period.

Figure 5 B_n vs. B_Σ. a) is for the equinoctial period, 8/5-9/10, 1967, and for T = 200 min., b) is for the winter period, 11/5-12/15, 1967, and for T = 60 min.

Figure 6 Examples of significant ΔB magnitude at times when the interplanetary magnetic field has been southward for some time. On the OGO data plots the straight line is the satellite location and also the $\Delta B = 0$ axis. The scale lines project away from the $\Delta B = 0$ axis in the direction of positive ΔB and are labeled with the scale, altitude, and universal time.

Figure 7 A series of OGO-4 passes and the simultaneous values of the north-south component of the interplanetary magnetic field. The format of the OGO-4 plots is the same as Figure 6.

Figure 8 Simultaneous plots of the north-south component of the interplanetary magnetic field, the magnetic field at a high latitude observatory (AT), and the horizontal components of magnetic disturbance at eight low latitude observatories. Possible occurrences of DP2 fluctuations are shaded and labeled.

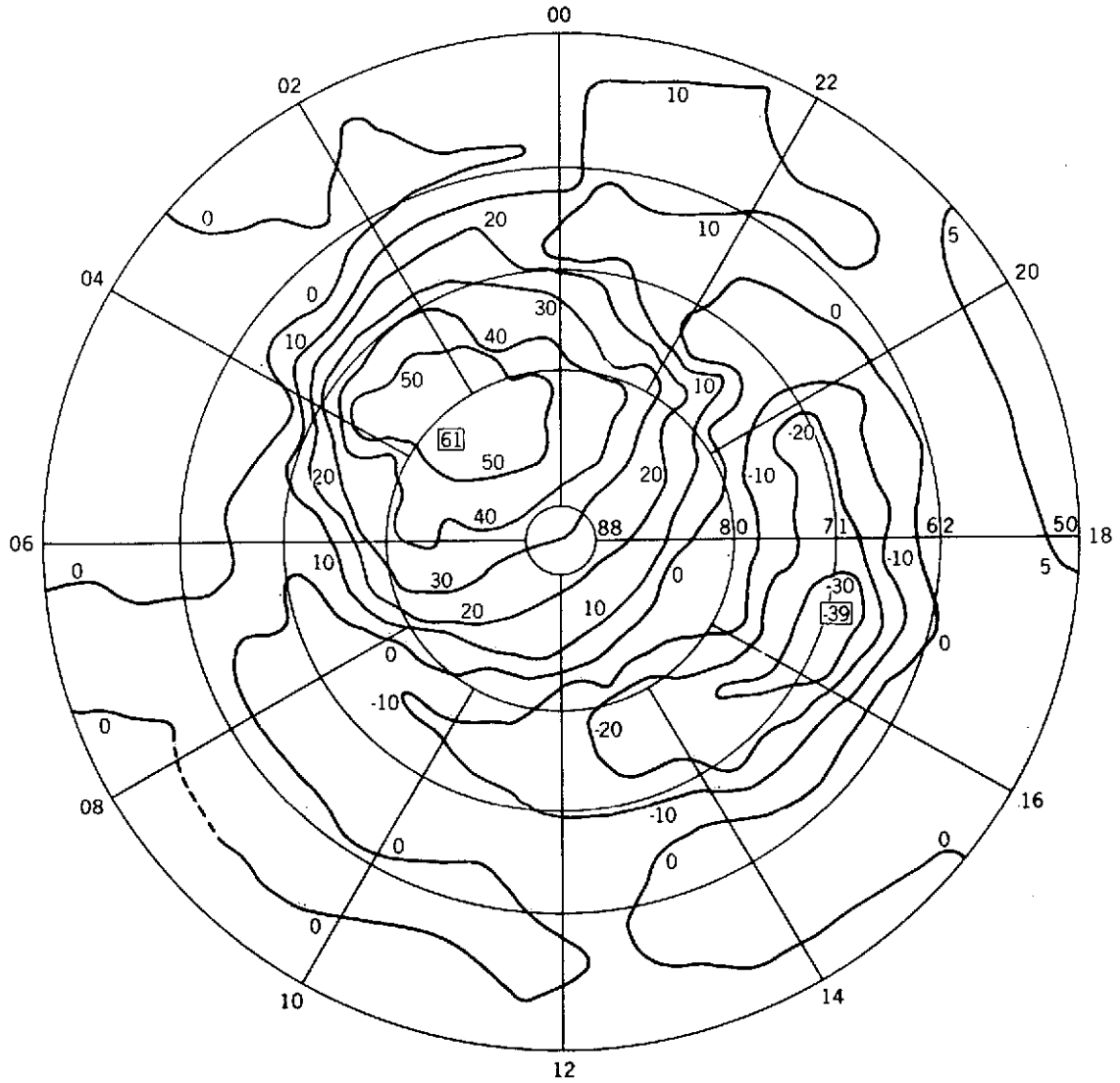

5 INDICATES HIGH OR LOW

Figure 1

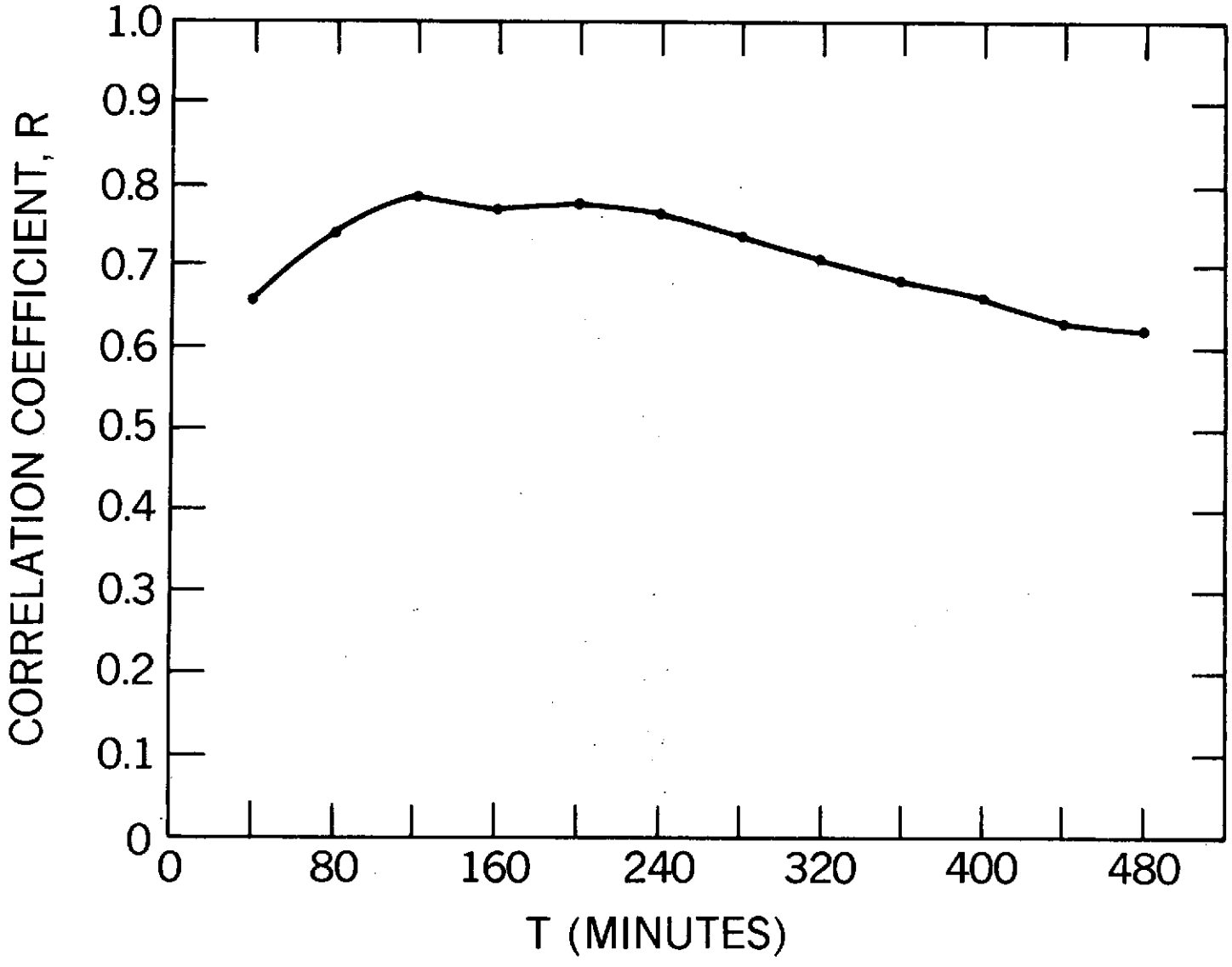
CORRELATION COEFFICIENT, R
1.0
0.9
0.8
0.7
0.6
0.5
0.4
0.3
0.2
0.1
0
0
80
160
240
320
400
480
T (MINUTES)

Figure 2

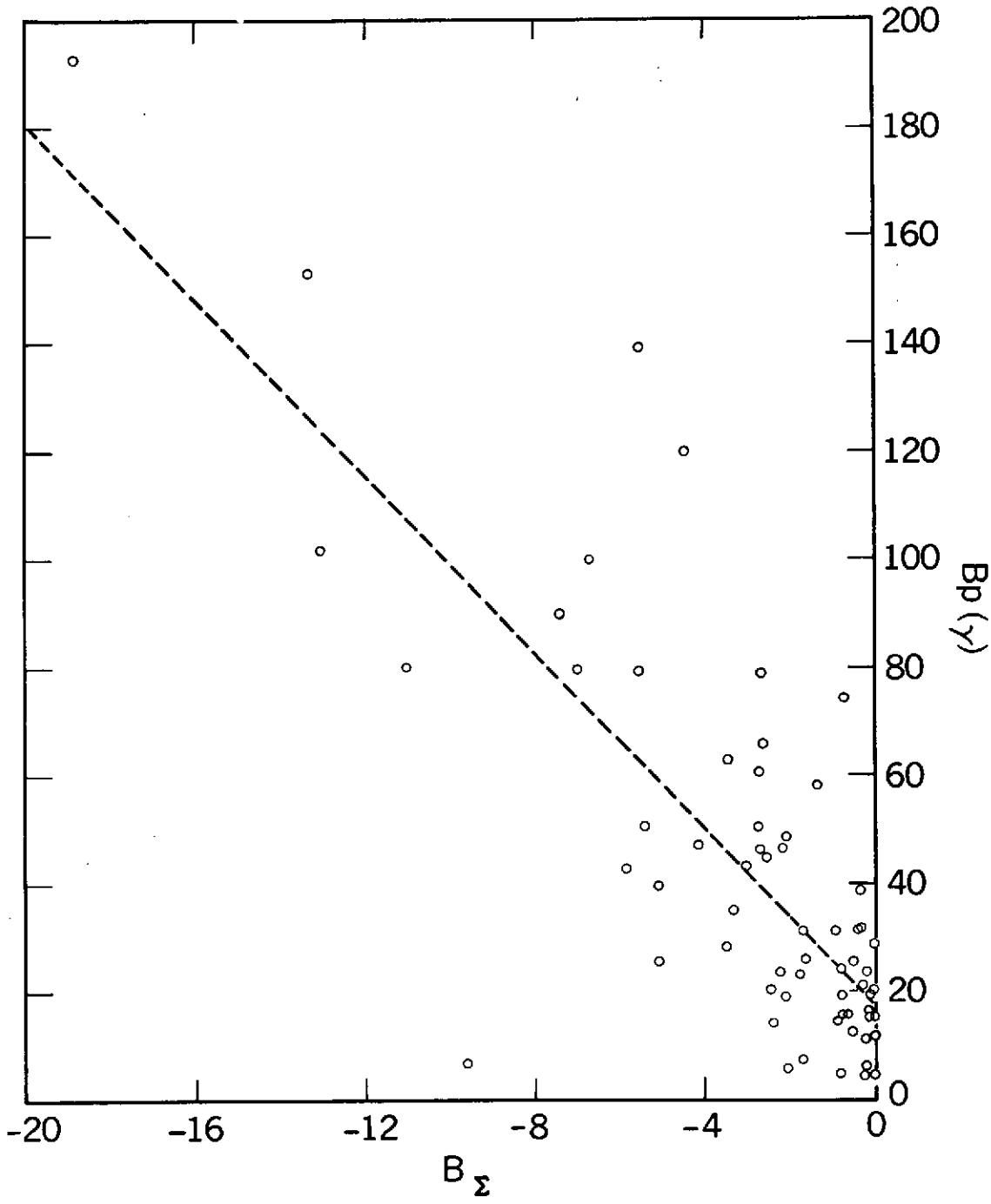

Figure 3a

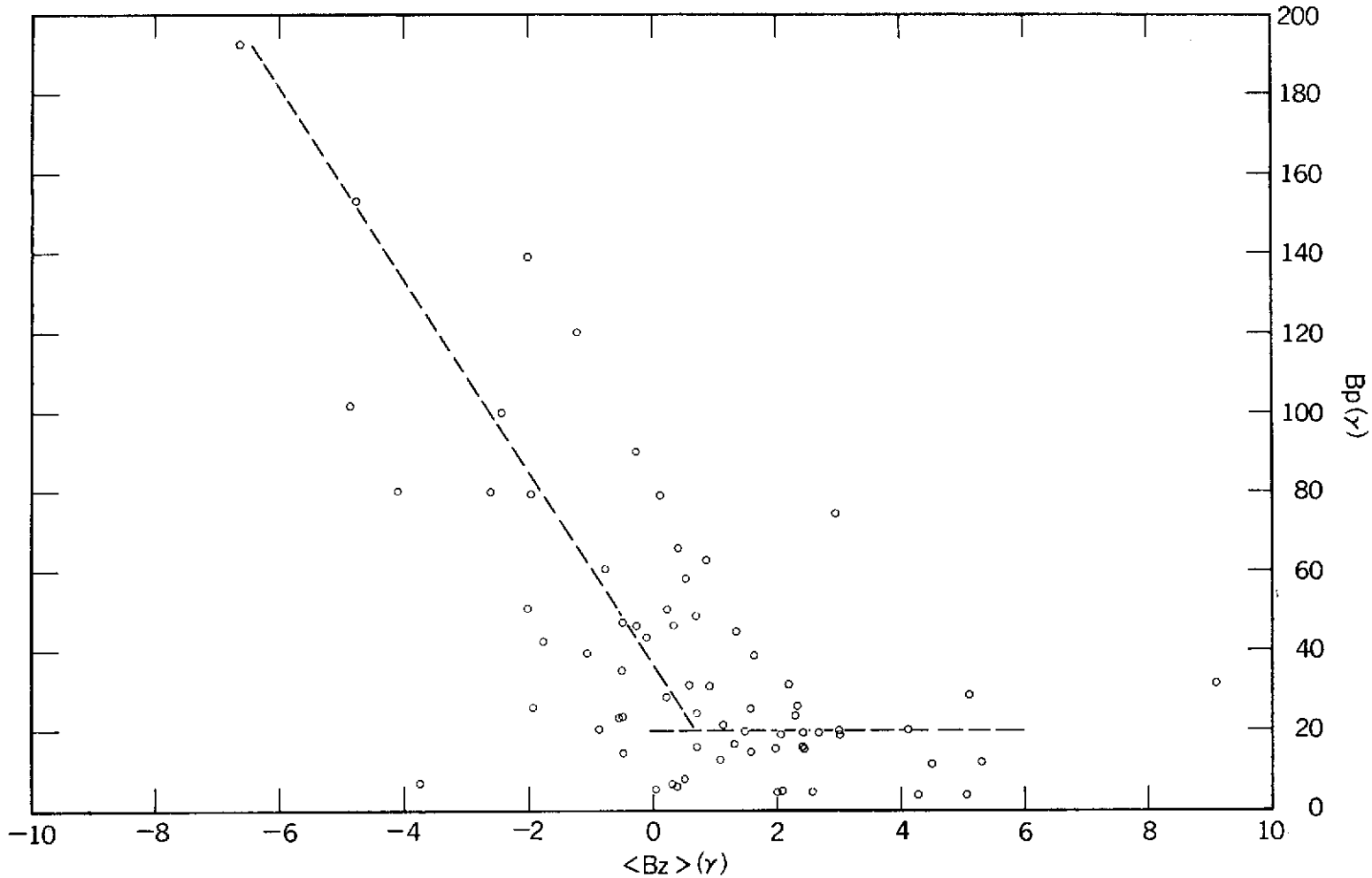

Figure 3b

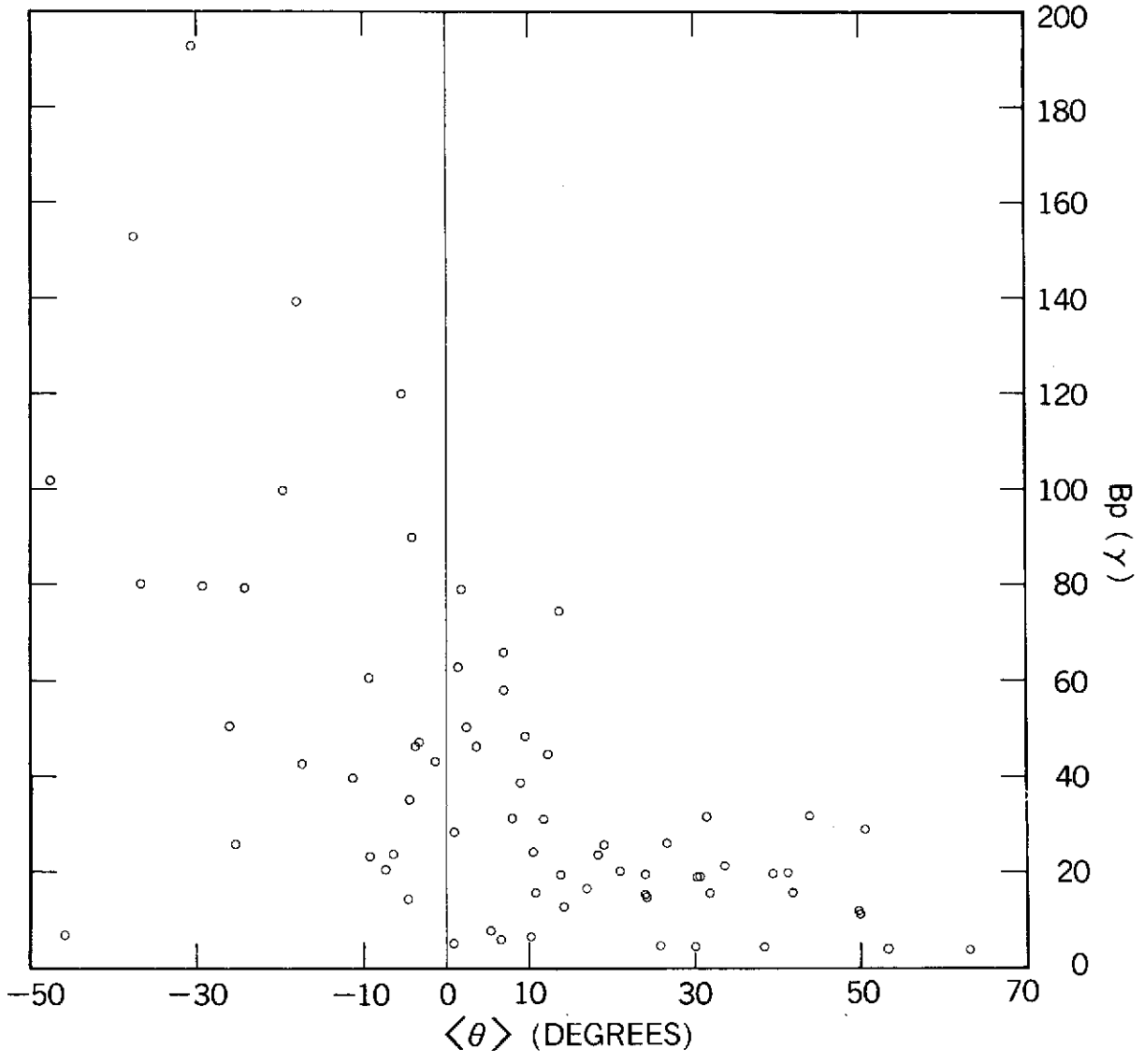
200
180
160
140
120
100
80
60
40
20
0
Bp (γ)
−50
−30
−10
0
10
30
50
70
⟨θ⟩ (DEGREES)

Figure 3c

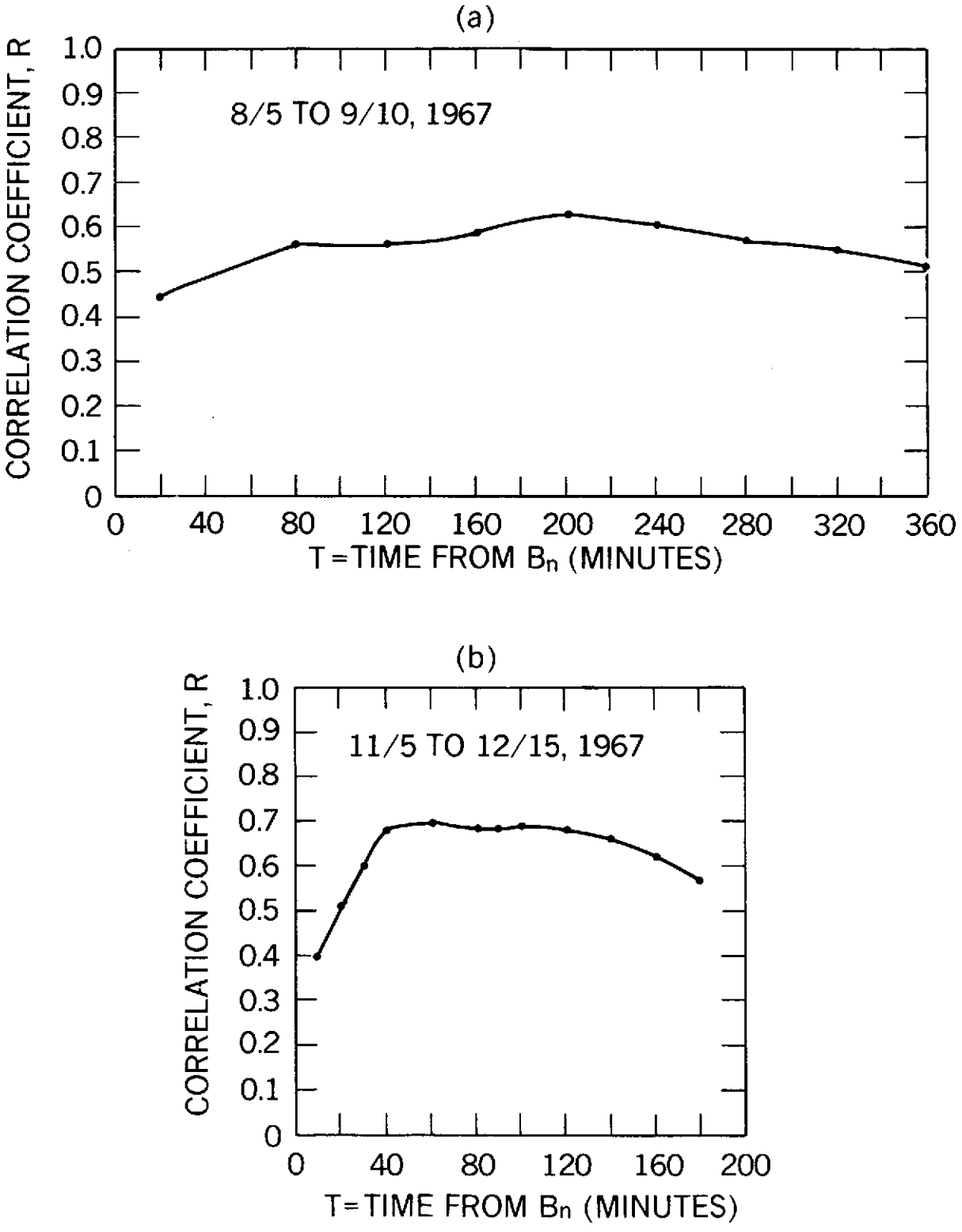
(a)
CORRELATION COEFFICIENT, R
1.0
0.9
0.8
0.7
0.6
0.5
0.4
0.3
0.2
0.1
0
8/5 TO 9/10, 1967
0
40
80
120
160
200
240
280
320
360
T = TIME FROM Bn (MINUTES)
(b)
CORRELATION COEFFICIENT, R
1.0
0.9
0.8
0.7
0.6
0.5
0.4
0.3
0.2
0.1
0
11/5 TO 12/15, 1967
0
40
80
120
160
200
T = TIME FROM Bn (MINUTES)

Figure 4

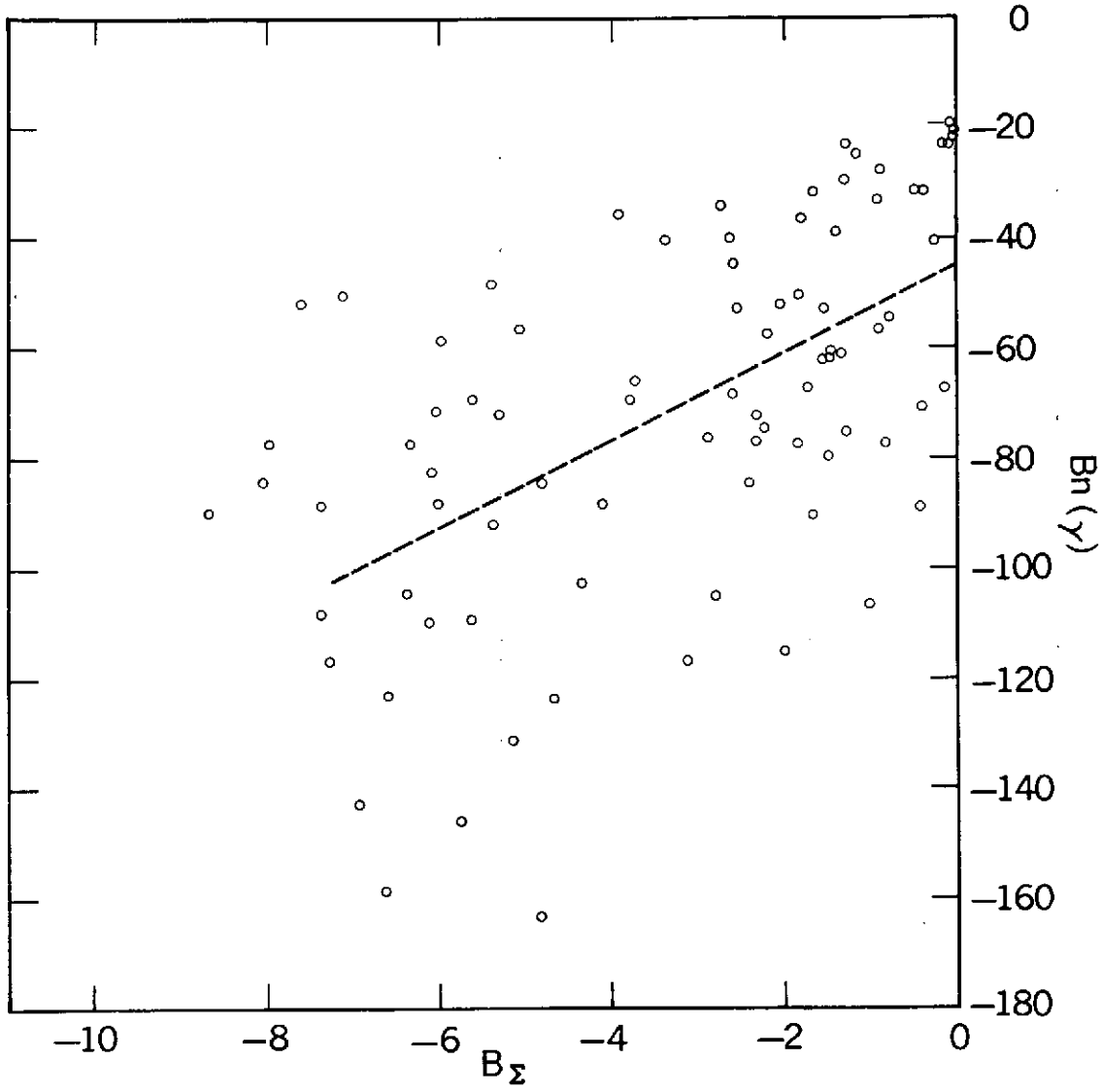

Figure 5a

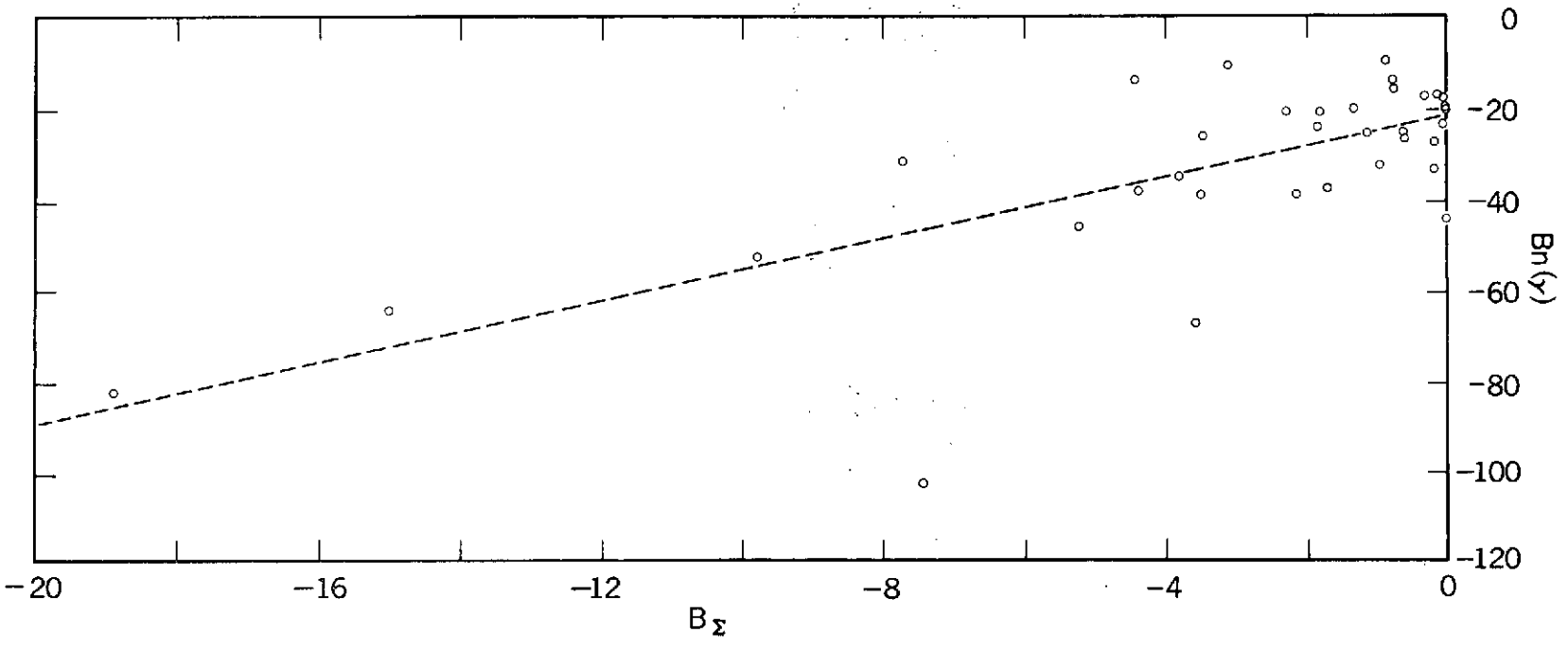

Figure 5b

OGO-4 POLAR PLOT
NORTHERN HEMISPHERE
7/29/67

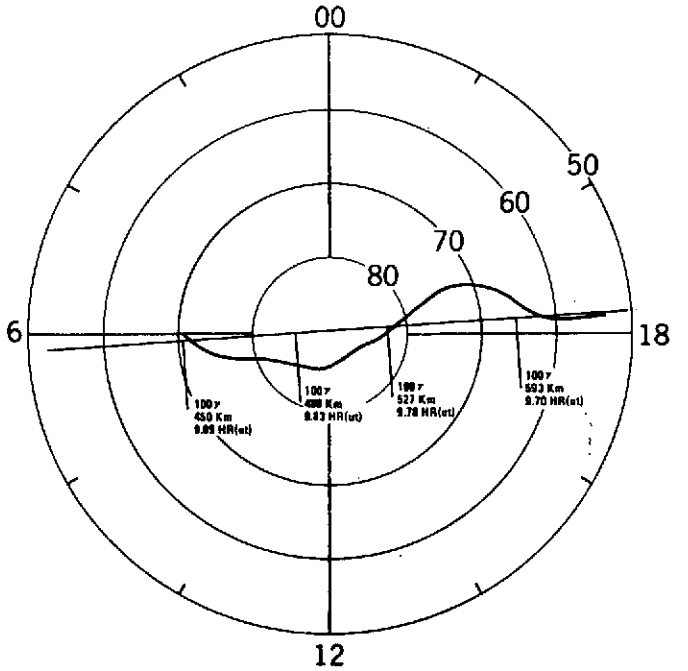

NORTH
COMPONENT OF
INTERPLANETARY
MAGNETIC FIELD

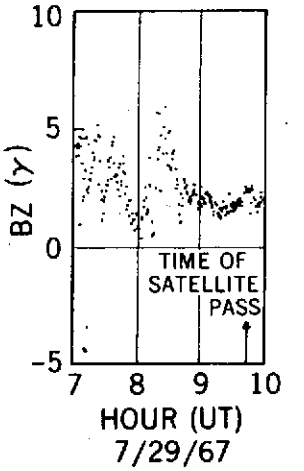

8/11/67

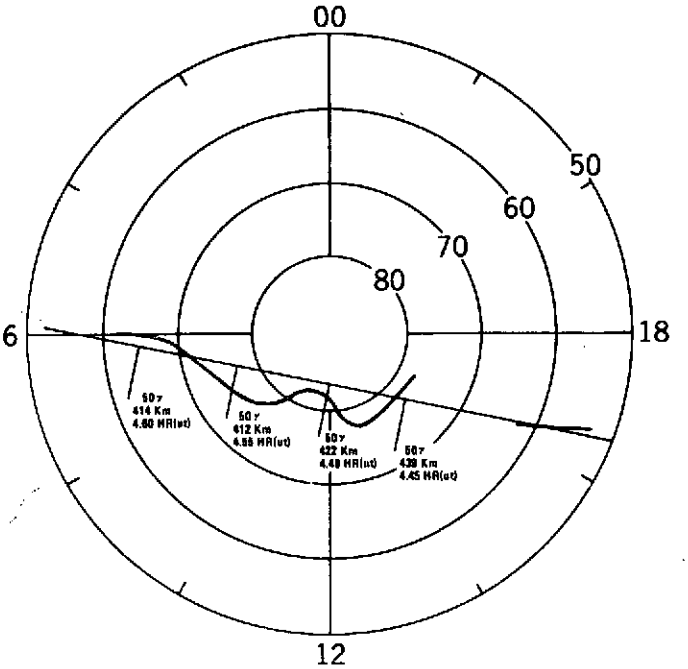

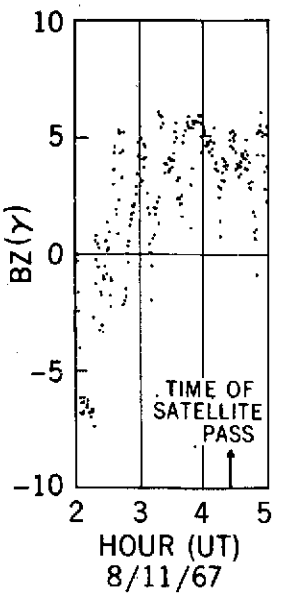

Figure 6

OGO-4 POLAR PLOTS
NORTH

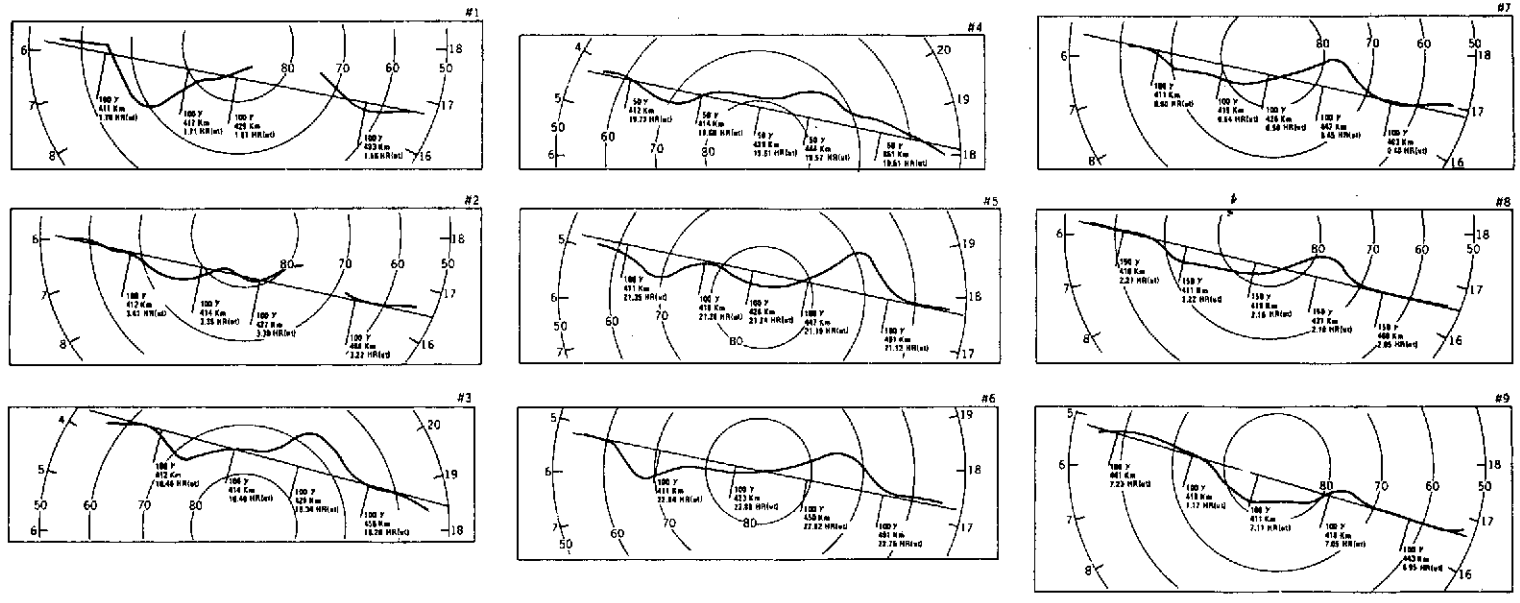

NORTH COMPONENT OF INTERPLANETARY MAGNETIC FIELD

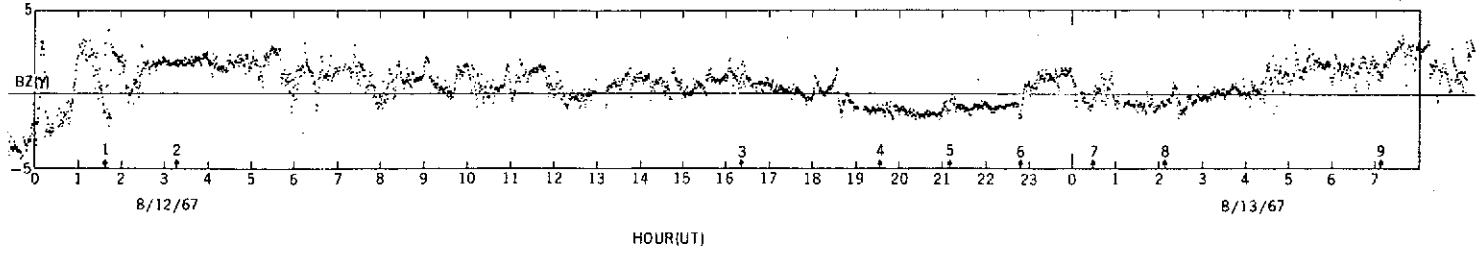

Figure 7

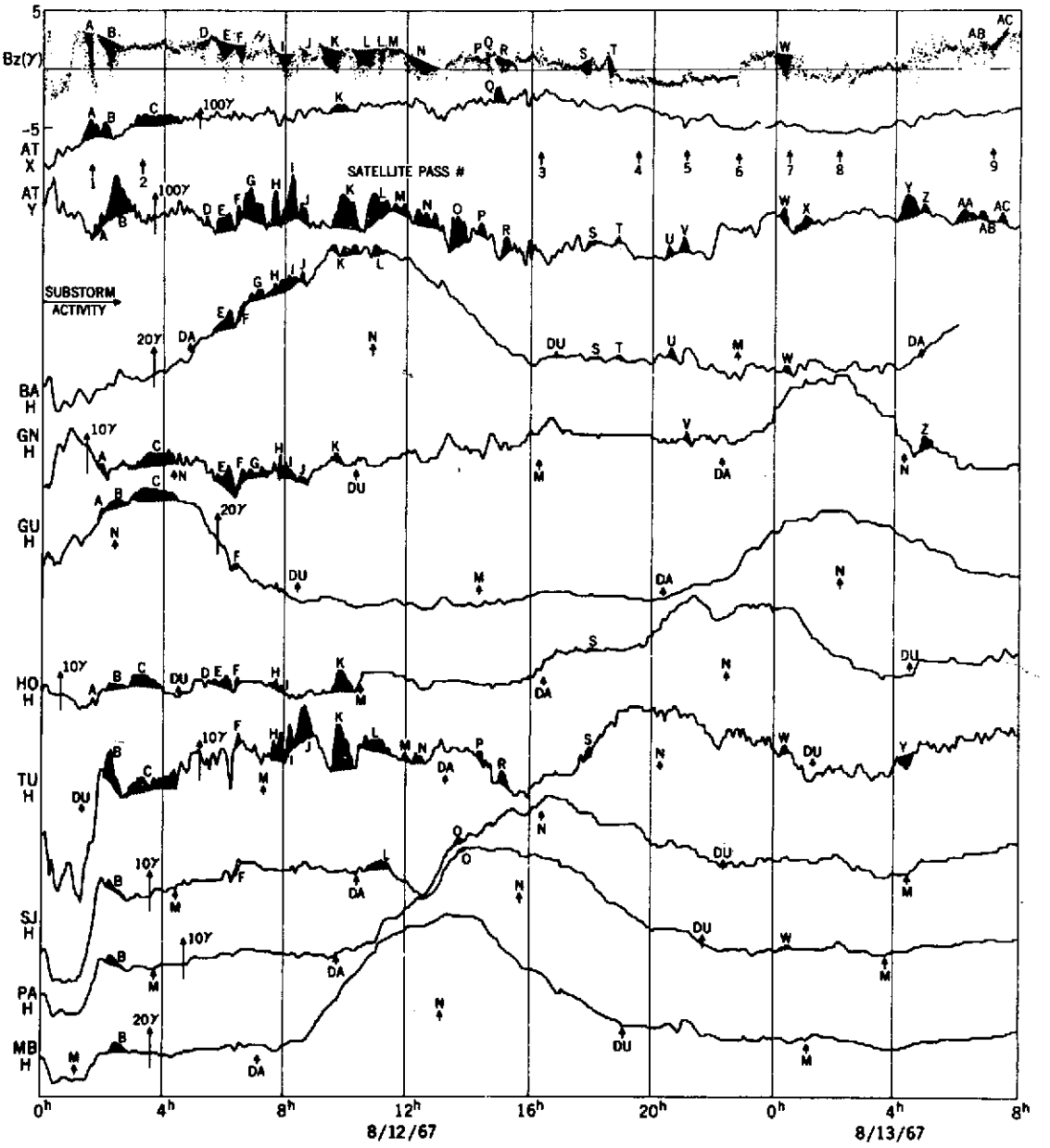
Bz(γ)
5
-5
AT X
AT Y
SATELLITE PASS #
SUBSTORM ACTIVITY
BA H
GN H
GU H
HO H
TU H
SJ H
PA H
MB H
0h
4h
8h
12h
16h
20h
0h
4h
8h
8/12/67
8/13/67

Figure 8